ISSN 1674-1056
http://cpb.iphy.ac.cn
http://iopscience.iop.org/cpb
中国物理 B
Chinese Physics
中国物理 Chinese Physics B

Thermal analysis of GaN-based laser diode mini-array

Jun-Jie Hu(胡俊杰), Shu-Ming Zhang(张书明), De-Yao Li(李德尧), Feng Zhang(张峰), Mei-Xin Feng(冯美鑫), Peng-Yan Wen(温鹏雁), Jian-Pin Liu(刘建平), Li-Qun Zhang(张立群), Hui Yang(杨辉)

Citation: Chin. Phys. B . 2018, 27(9): 094208. **doi:** 10.1088/1674-1056/27/9/094208

Journal homepage: http://cpb.iphy.ac.cn; http://iopscience.iop.org/cpb

What follows is a list of articles you may be interested in

High power external-cavity surface-emitting laser with front and end pump

Lidan Jiang(蒋丽丹), Renjiang Zhu(朱仁江), Maohua Jiang(蒋茂华), Dingke Zhang(张丁可), Yuting Cui(崔玉亭), Peng Zhang(张鹏), Yanrong Song(宋晏蓉)

Chin. Phys. B . 2018, 27(8): 084205. **doi:** 10.1088/1674-1056/27/8/084205

Novel single-transverse-mode control of VCSELs with dielectric mode filter

Lei Xiang(向磊), Xing Zhang(张星), Jian-Wei Zhang(张建伟), You-Wen Huang(黄佑文), Yong-Qiang Ning(宁永强), Li-Jun Wang(王立军)

Chin. Phys. B . 2018, 27(7): 074210. **doi:** 10.1088/1674-1056/27/7/074210

Broad bandwidth interference filter-stabilized external cavity diode laser with narrow linewidth below 100 kHz

Guan-Zhong Pan(潘冠中), Bao-Lu Guan(关宝璐), Chen Xu(徐晨), Peng-Tao Li(李鹏涛), Jia-Wei Yang(杨嘉炜), Zhen-Yang Liu(刘振杨)

Chin. Phys. B . 2018, 27(1): 014204. **doi:** 10.1088/1674-1056/27/1/014204

Different influences of u-InGaN upper waveguide on the performance of GaN-based blue and green laser diodes

Feng Liang(梁锋), De-Gang Zhao(赵德刚), De-Sheng Jiang(江德生), Zong-Shun Liu(刘宗顺), Jian-Jun Zhu(朱建军), Ping Chen(陈平), Jing Yang(杨静), Wei Liu(刘炜), Xiang Li(李翔), Shuang-Tao Liu(刘双韬), Yao Xing(邢瑶), Li-Qun Zhang(张立群), Mo Li(李沫), Jian Zhang(张健)

Chin. Phys. B . 2017, 26(11): 114203. **doi:** 10.1088/1674-1056/26/11/114203

Stable single-mode operation of 894.6 nm VCSEL at high temperatures for Cs atomic sensing

Lei Xiang(向磊), Xing Zhang(张星), Jian-Wei Zhang(张建伟), Yong-Qiang Ning(宁永强), Werner Hofmann, Li-Jun Wang(王立军)

Chin. Phys. B . 2017, 26(7): 074209. **doi:** 10.1088/1674-1056/26/7/074209

Thermal analysis of GaN-based laser diode mini-array*

Jun-Jie Hu(胡俊杰)[1,2], Shu-Ming Zhang(张书明)[1,†], De-Yao Li(李德尧)[1], Feng Zhang (张峰)[1], Mei-Xin Feng(冯美鑫)[1], Peng-Yan Wen(温鹏雁)[1], Jian-Ping Liu(刘建平)[1], Li-Qun Zhang(张立群)[1], and Hui Yang(杨辉)[1]

[1] *Key Laboratory of Nano-Devices and Applications, Suzhou Institute of Nano-Tech and Nano-Bionics, Chinese Academy of Sciences, Suzhou* 215123, *China*

[2] *University of Chinese Academy of Sciences, Beijing* 100049, *China*

(Received 3 April 2018; revised manuscript received 10 May 2018; published online 28 August 2018)

Thermal characteristics of multiple laser stripes integrated into one chip is investigated theoretically in this paper. The temperature pattern of the laser diode mini-array packaged in a TO-can is analyzed and optimized to achieve a uniform temperature distribution among the laser stripes and along the cavity direction. The temperature among the laser stripes varies by more than 5 K if the stripes are equally arranged, and can be reduced to less than 0.4 K if proper arrangement is designed. For conventional submount structure, the temperature variation along the cavity direction is as high as 7 K, while for an optimized trapezoid submount structure, the temperature varies only within 0.5 K.

Keywords: GaN laser diode, laser diode array, thermal analysis, temperature distribution

PACS: 42.55.Px **DOI:** 10.1088/1674-1056/27/9/094208

1. Introduction

In recent years, high power and high wavelength stability GaN-based blue laser diodes (LDs) have drawn great attention due to their potential applications in laser display and lightening.[1–3] Instead of watt-class single stripe laser diodes, integrating multiple stripes into one single chip to constitute an LD array is an effective way to achieve high output power.[4–7] Usually, the LD chips are packaged in a TO-can to realize electrical pumping and thermal dissipation. However, for an LD array, the temperature in each stripe can vary because the stripes are not thermally independent.[8,9] Careful consideration should be taken to optimize the arrangement of the stripes to achieve a uniform temperature distribution among the stripes. Furthermore, there is an inherent disadvantage for conventional TO package. Due to the asymmetric structure of the TO-can, the heat dissipation of the area close to the rear cavity facet is more effective than that of the area close to the front cavity facet. The temperature within the chip is not uniform along the cavity direction.[10] The nonuniformity of temperature among the stripes and along the cavity direction may deteriorate the wavelength stability, output power of LDs, and the device reliability.[5,11,12]

In this paper, the thermal characteristics of a GaN-based LD mini-array (with 5 laser stripes) in a TO-9 package is analyzed by using finite element method (FEM). Based on the analysis results, the arrangement of stripes is studied and optimized numerically to enhance the temperature uniformity. The influences of different submount structures are compared, and the temperature uniformity can be significantly improved if a trapezoid AlN submount is used.

2. Simulation model

The following heat conduction equation is numerically solved for the analysis of thermal characteristics of the GaN based LD mini-array in a TO-9 package.

$$\rho c \frac{\partial T}{\partial t} = qv + k\nabla^2 T, \tag{1}$$

where T is the temperature, ρ is the density, c is the specific heat, t is the time, qv is the heat source density, and k is the thermal conductivity.[13] In this work, the numerical calculation of Eq. (1) is solved in three dimensions by the finite element method.

Three-dimensional TO-9 packaged LD mini-array model is built for thermal simulation. Figure 1 shows the schematic structure of the TO-9 packaged LD. The GaN-based LD mini-array chip is mounted on an AlN submount. The AlN submount is then attached on a copper heat sink. AuSn solder is used to bond the LD mini-array chip, the AlN submount, and the copper heat sink. Figure 2 shows the schematic structure of the LD mini-array chip. The width of the LD mini-array chip is 500 μm and the cavity length is 1200 μm. In the middle of the chip is a 100 μm wide emitting area, which consists of five

*Project supported by the National Key Research and Development Program of China (Grant Nos. 2016YFB0402002, 2016YFB0401803, 2017YFB0405002, 2017YFB0405003, and 2017YFB0405005), the National Natural Science Foundation of China (Grant Nos. 61574160, 61704184, and 61334005), the Strategic Priority Research Program of the Chinese Academy of Science (Grant No. XDA09020401), the Chinese Academy of Science Visiting Professorship for Senior International Scientists (Grant No. 2013T2J0048), the Natural Science Foundation of Jiangsu Province, China (Grant No. BK20170430), and the CPSF-CAS Joint Foundation for Excellent Postdoctoral Fellows, China (Grant No. 2016LH0026).

†Corresponding author. E-mail: smzhang2010@sinano.ac.cn

© 2018 Chinese Physical Society and IOP Publishing Ltd

laser stripes (stripe 1–5). The structural parameters *rw*1, *rw*2, *rw*3, *rw*4, and *rw*5 represent the width of each stripe; *s*1, *s*2, *s*3, and *s*4 represent the spacing between the stripes.

Table 1 shows the material parameters used in the thermal simulation. We suppose that the wall plug efficiency (WPE) of the LD mini-array is 30%, and the input power is set to 10 W, which means that the optical power is 3 W and the thermal power is 7 W. In GaN based LDs, except for the active region, the heat generation in the P-cladding layer is also large,[14] so we assume that the thermal power is uniformly distributed in the active layer and the P-cladding layer of each stripe. The stem in the TO-9 package is supposed to be seated on a thermoelectric cooler (TEC), and the temperature is fixed to 300 K.

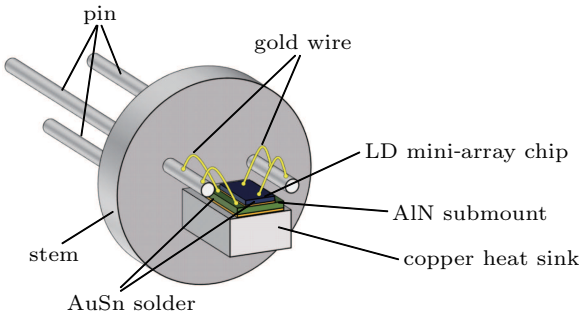


Fig. 1. (color online) Schematic diagram of a GaN-based LD mini-array in a TO-9 package.

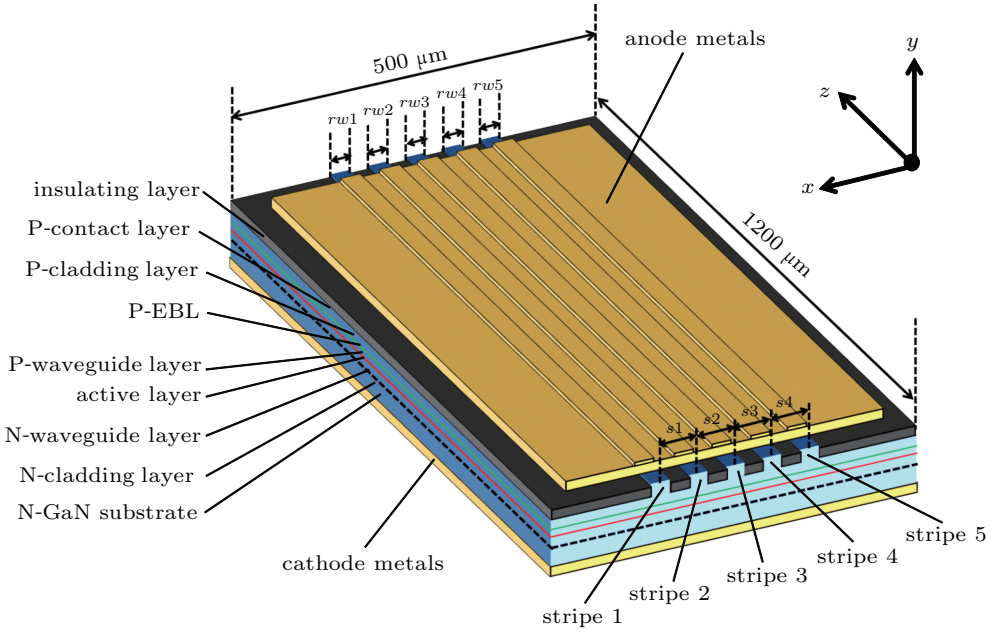


Fig. 2. (color online) Schematic diagram of a GaN-based LD mini-array chip with five stripes.

Table 1. Material parameters in the simulation at 300 K.

	Component in the packaged structure	Material	Thermal conductivity /W·mK^{-1}
1	stem	copper	397
2	heat sink	copper	397
3	solder	AuSn	57
4	submount	AlN	170
5	substrate	GaN	130
6	N-cladding layer	AlGaN	20
7	N-waveguide layer	InGaN	20
8	active layer	InGaN/GaN MQWs	70
9	P-waveguide layer	InGaN	70
10	P-EBL	AlGaN	70
11	P-cladding layer	AlGaN	20
12	P-contact layer	GaN	20
13	insulating layer	SiO_2	1.4
14	anode	Au	317
15	cathode	Au	317

3. Results and discussion

By using the parameters mentioned above, we calculated the temperature distribution of a GaN based LD mini-array in a TO-9 package, as shown in Fig. 3. In the middle of the chip is a 100 μm wide emitting area, in which five 10 μm wide laser stripes are uniformly spaced. We extracted the temperature data among the stripes and along the cavity direction (along the *x*-axis and along the *z*-axis), as shown in the inset of Fig. 3. It is found that among the stripes, higher temperatures locate in the middle stripes, while along the cavity direction, temperatures near the front cavity facet is higher than that near the rear cavity facet. The close spacing causes serious thermal crosstalk between the stripes, which leads to a nonuniform temperature distribution among the stripes. The rear cavity facet is closer to the stem (seated on a TEC), which also leads to a nonuniform temperature distribution along the cavity direction.

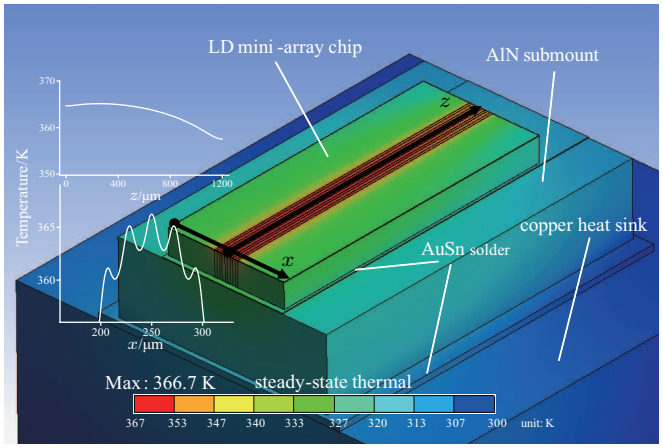


Fig. 3. (color online) Temperature distributions of GaN-based LD mini-array in a TO-9 package. The inset is the extracted temperature data along the *x*-axis and the *z*-axis.

To improve the temperature uniformity of the LD mini-array chip, the temperature distribution among the stripes and along the cavity direction is separately optimized by reasonable arrangement of the stripes and the structure of AlN submount. Details are discussed in the following sections.

3.1. Optimization of the temperature distribution among the stripes

Figure 4 shows the schematic diagram of the emitting area, and the structural parameters *rw*1–*rw*5 and *s*1–*s*4 are signed in the diagram. Four sets of structural parameters are listed in Table 2, namely P1, P2, P3, and P4, and figure 5 is the corresponding temperature among the stripes (*x*-axis direction) extracted from the simulation results when using different sets of structural parameters. The parameters of P1 represent the conventional structure in which five 10 μm stripes are equally spaced in the emitting area. The temperatures of the middle stripes are higher than those of the stripes in both sides, and the temperature varies by more than 5 K. Firstly, we enlarge the spacing *s*2 and *s*3 from 22.5 μm to 26 μm, and reduce the spacing *s*1 and *s*4 from 22.5 μm to 19 μm, as shown by P2 in Table 2. Compared with using structural parameters of P1, the temperatures of the stripes in the middle decrease and the temperatures of the side ones increase, and the temperature difference is reduced to 3 K. Then we continue to increase *s*2 and *s*3 to 28 μm and reduce *s*1 and *s*3 to 17 μm, as shown by P3 in Table 2. The temperatures of stripe 2, stripe 3, and stripe 4 become similar, but the temperatures of stripe 1 and stripe 5 are still low, and the temperature difference is reduced to 2.5 K. It is difficult to achieve a uniform temperature distribution among stripes via adjusting the spacing only. At last, based on the parameters of P2, we decrease the widths of stripe 2, stripe 3, and stripe 4, and increase the widths of stripe 1 and stripe 5, as shown by P4 in Table 2. Parameters *rw*3, *rw*4, and *rw*2 are reduced to 8.5 μm, 8.25 μm, and 8.25 μm, and *rw*1 and *rw*5 are increased to 12.5 μm, while the total width of the stripes is still 50 μm (keep the same heat power generated at the emitting area). The temperatures of all stripes become similar and the temperature difference is reduced to less than 0.4 K.

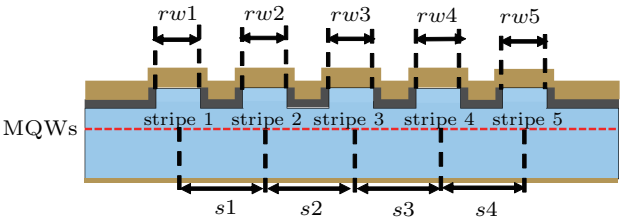


Fig. 4. (color online) Schematic diagram of emitting area in the GaN based LD mini-array chip.

Table 2. Structural parameters in μm.

	*rw*1	*s*1	*rw*2	*s*2	*rw*3	*s*3	*rw*4	*s*4	*rw*5
P1	10	22.5	10	22.5	10	22.5	10	22.5	10
P2	10	19	10	26	10	26	10	19	10
P3	10	17	10	28	10	28	10	17	10
P4	12.5	19	8.25	26	8.5	26	8.25	19	12.5

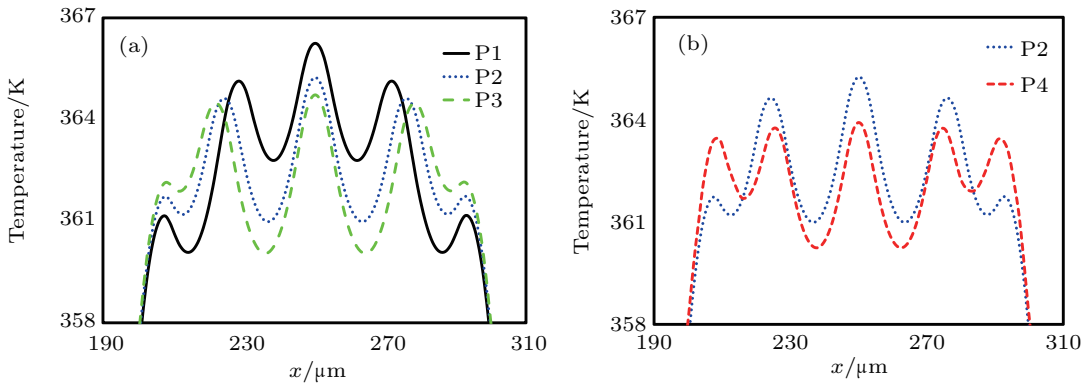


Fig. 5. (color online) Temperature distribution among the stripes (*x*-axis direction) with different structural parameters: (a) P1, P2, and P3, (b) P2 and P4.

Compared with using structural parameters of P1, adopting structural parameters of P4, as shown in Fig. 6, can significantly improve the temperature uniformity of the stripes, while the highest temperature decreases from 367.7 K to 364.4 K.

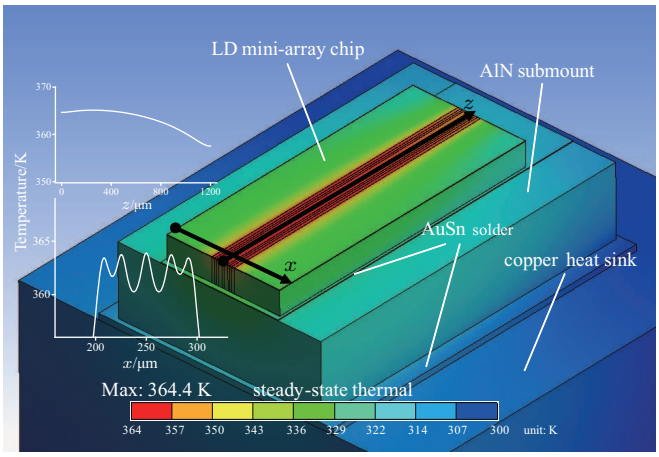


Fig. 6. (color online) Temperature distributions of GaN-based LD mini-array in a TO-9 package using structural parameters of P4. The inset is the extracted temperature data along the x-axis and the z-axis.

3.2. Optimization of the temperature distribution along the cavity direction

As mentioned above, the temperature along the cavity direction (z-axis direction) is also nonuniform. As shown in Fig. 6, the temperature near the front cavity facet is higher than that near the rear cavity facet. We have changed the structure of AlN submount to improve the temperature distribution. The idea is to enlarge the volume of the AlN submount near the front cavity facet to dissipate more heat, while reduce the volume of the AlN submount near the rear cavity facet to improve the temperature uniformity near the rear facet.

Figures 7 and 8 show four different AlN submount structures and their corresponding temperature distributions along the cavity direction, respectively. The thicknesses of the AlN submount used are all set to 300 μm,[15] but the shapes vary. Figure 7(a) shows 900 μm×1400 μm rectangular AlN submount, which is conventionally used in the TO-9 package. In our simulation results, the temperature difference along the z-axis can be 7.6 K. In Fig. 7(b), triangular AlN submount is used in simulation model. Since the upper surface size of the copper heat sink in TO-9 package is 1850 μm×1750 μm, we set the width in front to 1650 μm and the length to 1800 μm (50 μm reserved for AuSn solder). The overall temperature is reduced due to the increase in the volume of AlN submount, and the temperature difference along the z-axis is reduced to 5.5 K, which is still large. In Fig. 7(c), we cut off the volume of the triangular AlN submount near the rear cavity facet, and the length of the AlN submount is reduced to 1400 μm. The shape of the AlN submount becomes a trapezoid column and the temperature difference is reduced to 4.5 K. In Fig. 7(d), the volume behind is further reduced until the length of the AlN submount is 1210 μm. The overall temperature slightly increases but the highest temperature is still lower than that using the conventional rectangular AlN submount, and the temperature difference along the z-axis is only 0.5 K.

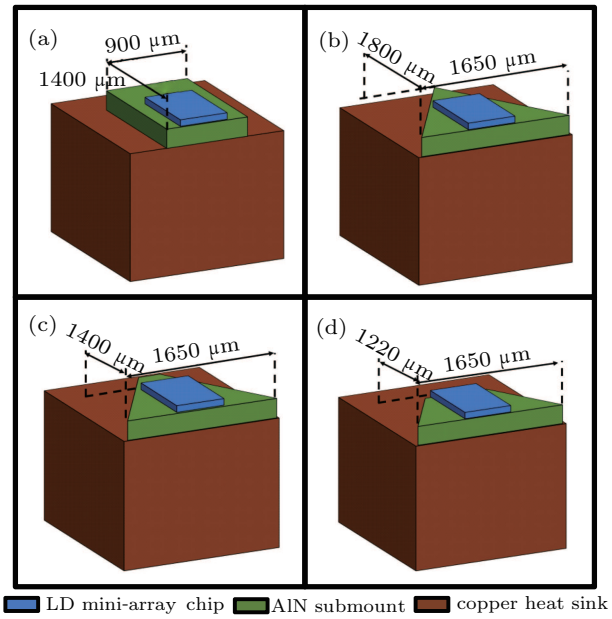


Fig. 7. (color online) Schematic diagram of different AlN submount structures. (a) Rectangular AlN submount. (b) Triangular AlN submount. (c) and (d) Trapezoid AlN submount.

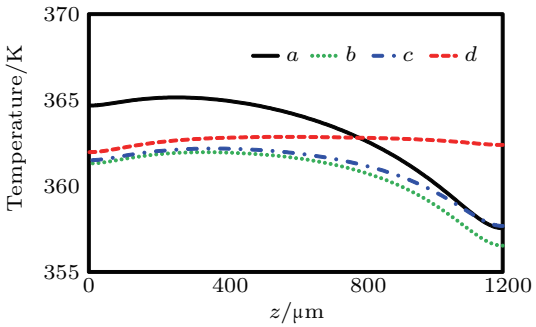


Fig. 8. (color online) Temperature distribution along the cavity direction (z-axis direction) with different AlN submount structures. Curves a, b, c, and d correspond to Figs. 7(a), 7(b), 7(c), and 7(d), respectively.

3.3. Temperature distribution under different input powers

By optimizing the structural parameters and using a trapezoid AlN submount, the temperature difference among the stripes and along the cavity direction are less than 0.4 K and 0.5 K, respectively, as shown in Fig. 9. The temperature distribution of the LD mini-array operating under different input powers is also simulated by the model described above, as shown in Fig. 10. The input power is set to be 3.33 W, 6.67 W, 10 W, and 13.33 W, respectively. Although the overall temperature on the ridge is increased with the increase of the thermal power, the temperature difference among the stripes is within 0.7 K, while the temperature difference along the cavity direction is within 1 K.

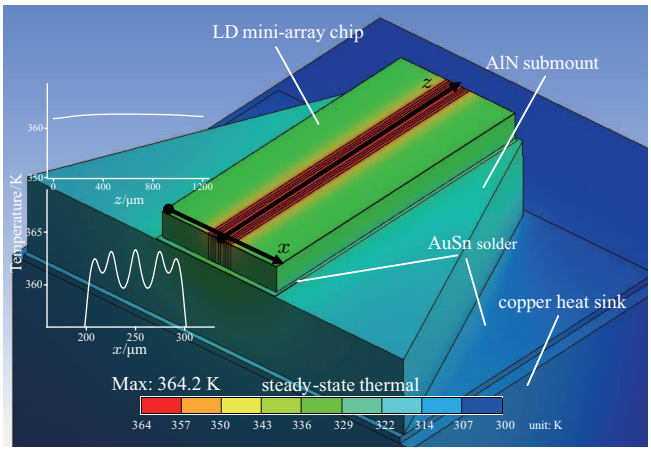


Fig. 9. (color online) Temperature distribution of GaN-based LD mini-array in a TO-9 package using structural parameters of P4 and a trapezoid AlN submount. The inset is the extracted temperature data along the x-axis and the z-axis.

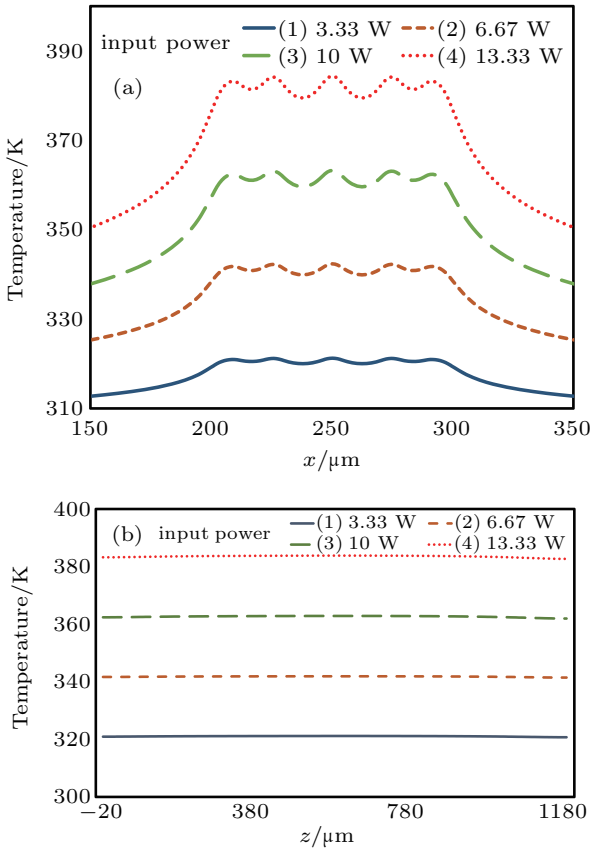


Fig. 10. (color online) Temperature distribution under different thermal power (a) among stripes; (b) along the cavity direction.

4. Conclusion

We have calculated the temperature pattern of a GaN-based LD mini-array with 5 stripes in a TO-9 package and optimized the temperature distribution by reasonable arrangement of the stripes and using the trapezoid AlN submount. From the analyses it is suggested that the temperature distribution among the stripes can be adjusted by the widths of stripes and the spacing between stripes, and the temperature distribution along the cavity direction can be adjusted by optimizing the structure of AlN submount. When the input power of LD mini-array is 10 W, by using the optimal structural parameters and a trapezoid AlN submount, the temperature variation among stripes is less than 0.4 K and along the cavity direction is less than 0.5 K. Meanwhile, comparing with the conventional structure, the highest temperature decreases from 366.7 K to 364.2 K. Regardless of the variation of the input power, the temperature fluctuations among stripes and along cavity direction are always within controllable range. As a result, the lasing wavelength uniformity and the reliability of the GaN based LD mini-array can be improved.

References

[1] Hwang W J, Lee T H, Nam O H, Kim H K, Kwak J S, Park Y J and Shin M W 2006 *Phys. Status Solidi C* **3** 2174

[2] Ji L, Jiang D S, Zhang S M, Liu Z S, Zheng C, Zhao D G, Zhu J J, Wang H, Duan L H and Yang H 2010 *Chin. Phys. B* **19** 124211

[3] Gmachl C F, Asano T, Bour D P, Takeya M, Mizuno T, Ikeda S, Ohfuji Y, Fujimoto T, Oikawa K, Goto S, Hashizu T, Aga K and Ikeda M 2004 *Proc. SPIE* **5365** 297

[4] Goto S, Ohta M, Yabuki Y, Hoshina Y, Naganuma K, Tamamura K, Hashizu T and Ikeda M 2003 *Phys. Status Solidi A* **200** 122

[5] Perlin P, Marona L, Holc K, Wisniewski P, Suski T, Leszczynski M, Czernecki R, Najda S, Zajac M and Kucharski R 2011 *Appl. Phys. Express* **4** 062103

[6] Ji L, Zhang S M, Jiang D S, Li Z S, Zhang L Q, Zhu J J, Zhao D G, Duan L H and Yang H 2010 *Chin. Phys. Lett.* **27** 054204

[7] Chen P, Zhao D G, Feng M X, Jiang D S, Liu Z S, Zhang L Q, Li D Y, Liu J P, Wang H, Zhu J J, Zhang S M, Zhang B S and Yang H 2013 *Chin. Phys. Lett.* **30** 104205

[8] Zhang Z Y, Zhang P, Nie Z Q, Li X N, Xiong L L, Liu H, Wang Z F and Liu X S 2013 *High Power Laser Part. Beams* **25** 1904

[9] Belyanin A A, Samonji K, Smowton P M, Yoshida S, Hagino H, Yamanaka K and Takigawa S 2012 *Proc. SPIE* **8277** 82771K

[10] Shi D, Feng S, Qiao Y and Wen P Y 2015 *SolidState Electron.* **109** 25

[11] Perlin P, Świetlik T, Marona L, Czernecki R, Suski T, Leszczyński M, Grzegory I, Krukowski S, Nowak G, Kamler G, Czerwinski A, Plusa M, Bednarek M, Rybiński J and Porowski S 2008 *J. Cryst. Growth* **310** 3979

[12] Ryu H Y, Ha K H, Chae J H, Nam O H and Park Y J 2005 *Appl. Phys. Lett.* **87** 093506

[13] Zhu C, Zhang Y G, Li A Z and Tian Z B 2006 *J. Appl. Phys.* **100** 053105

[14] Hatakoshi G, Onomura M, Yamamoto M, Nunoue S Y, Itaya K and Ishikawa M 1999 *Jpn. J. Appl. Phys.* **38** 2764

[15] Feng M X, Zhang S M, Jiang D S, Liu J P, Wang H, Zeng C, Li Z C, Wang H B, Wang F and Yang H 2012 *Chin. Phys. B* **21** 084209